Solar-Panel Integrated Circularly Polarized Meshed Patch for Cubesats and Other Small Satellites

IEEE Access
Multidisciplinary : Rapid Review : Open Access Journal

Date of publication xxxx 00, 0000, date of current version xxxx 00, 0000.

Digital Object Identifier 10.1109/ACCESS.2017.DOI

Solar-Panel Integrated Circularly Polarized Meshed Patch for CubeSats and Other Small Satellites

SYMON K. PODILCHAK[1], (Member, IEEE,) DAVIDE COMITE[2], (Member, IEEE), BRENDAN K. MONTGOMERY[3], (Student Member, IEEE), YUEPEI LI[1], (Student Member, IEEE), VICTORIA GÓMEZ-GUILLAMÓN BUENDÍA[1], (Member, IEEE), and YAHIA M. M. ANTAR[3], (Life Fellow, IEEE)

[1]Institute of Sensors, Signals, and Systems, School of Engineering and Physical Sciences, Heriot-Watt University, Edinburgh, Scotland, EH14 4AS (e-mail: skp@ieee.org)

[2]Department of Information Engineering, Electronics and Telecommunications, Sapienza University of Rome, 00184 Rome, Italy (e-mail: davide.comite@uniroma1.it)

[3]Department of Electrical and Computer Engineering, The Royal Military College of Canada, Kingston, Ontario (e-mail: antar-y@rmc.ca).

Corresponding author: Symon K. Podilchak (e-mail: skp@ieee.org).

This work was supported by the European Union's Horizon 2020 Research and Innovation Program through Marie Sklodowska-Curie under Grant 709372

ABSTRACT This paper presents the design of a circularly polarized (CP) meshed patch antenna fully integrated within a solar panel for operation on CubeSats and other microsatellites. The structure has been designed to ensure optimal antenna performance at S band as well as to minimize any shadowing effects that can reduce the received power at the solar cells. To generate CP the antenna is driven by two orthogonal feed points, penetrating through a transparent borosilicate glass layer as well as a silicon and PCB substrate. Simulated and measured performances, on both a preliminary FR4 design and a fully integrated prototype, demonstrate good impedance bandwidth, satisfactorily axial ratio, as well as stable radiation patterns and minimum shadowing levels. The proposed antenna can be useful for communications between satellites as well as with the ground station, and since the structure is compact and completely integrated, the design can be an alternative approach to new phased arrays on solar panels and other beam-steering systems.

INDEX TERMS Planar antennas, circular polarization, CubeSat, meshed patch, transparent antennas.

I. INTRODUCTION AND BACKGROUND

The need for directional, wideband, and compact antennas for earth observation and space communications requires advanced and well-integrated design solutions. Small satellites, such as those conforming to the CubeSat standard [1]–[3], are typically designed to maximize the solar panel surface area, which is critical for efficient solar power harvesting and to enable long-term operation of the space vehicle. Therefore, the elimination of antenna shadowing, caused by the obstruction of any incident light onto the solar cells due to the antenna placement, is imperative and it should not be accomplished at the cost of reduced antenna performance [4].

Increasing efforts have been devoted, in the last decade, to the design of high-performance conformal antennas aboard small satellites [5] and of quasi-transparent patch antennas positioned over the surface of solar panels [4], [6], [7]. In this frame, we propose here a novel configuration of a dual-fed circularly polarized (CP) square patch antenna fully integrated on a transparent glass substrate and solar cell layer for placement on satellite (see Figs. 1-3). The proposed meshed patch is designed to operate in the S band and it can also be useful for phased-array systems and communications between more conventional satellites as well as for other small spaceborne platforms. To the best knowledge of the authors, no similar CP meshed patch antenna has been fully integrated within a commercial solar panel for small satellite applications.

Meshed antennas operate on the same principle as conventional microstrip patches [8], [9], [10], the only difference being the minimal use of metallization on the top layer without significantly compromising the radiation performance, the bandwidth (BW), etc., of the antenna, while also maximizing its efficiency. If properly designed and optimized, meshed antennas can represent a valuable alternative with respect to

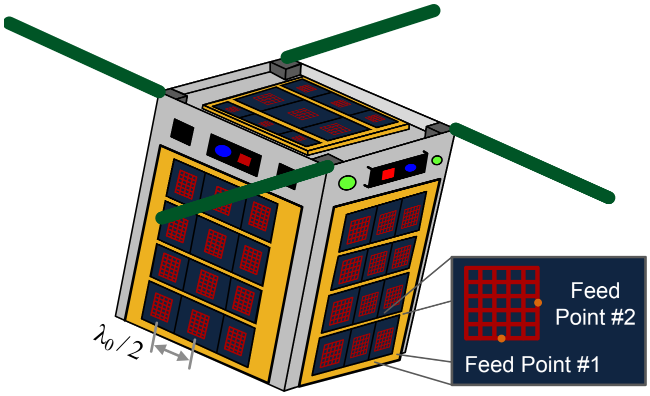

FIGURE 1. **Illustration of the proposed meshed patch antenna for solar panel integration and placement on CubeSats and other satellites. Two feed points enable CP radiation and the square patch can be placed on multiple solar panels (separated by about $\lambda_0/2$ where λ_0 is the free-space wavelength) forming an antenna array.**

different devices integrated around solar cells [6], [11]–[13].

At microwave frequencies, meshed solutions have been originally proposed for wireless communications to provide optical transparency in automotive applications, heterogeneous mesh networks, and for beamforming, where it is commonly desired to reduce the antenna visual or spatial impact (see, e.g., [14] and refs. therein). Different meshed patch designs have been recently reported in literature. For example, a single-feed CP design based on variable line widths of the mesh has been originally reported in [15], but it was optimized on a conventional PCB design and, thus, it was not integrated within a solar panel, whose presence can significantly alter the antenna performance. The 2.43 GHz design was also based on the excitation of degenerate modes by means of conventional single feed-point microstrip connectivity, achieving a maximum gain of 4.9 dB_{ic} with an impedance and axial ratio (AR) $\text{BW}_{3\,\text{dB}}$ of 6.54% and 2.79%, respectively.

A similar PCB design excited by proximity feeding was originally proposed in [16] and optimized in [17]. In that work a gain of 5.15 dB_{ic}, an impedance BW of 2%, and an AR $\text{BW}_{3\,\text{dB}}$ of 0.6%, at 2.47 GHz, were reported, at the cost of reduced transparency due to the use of coplanar proximity feeding. A dual-band patch antenna was also reported in [18] based on metamaterial loading to control the relative phase difference between the orthogonal modes supported by a single patch. The design achieved gain values equal to 4.4 dB_{ic} and 4.8 dB_{ic} at 2.35 GHz and 2.73 GHz, respectively, and an optical transparency equal to 70%.

Following these developments, a linear-polarized meshed patch antenna for integration with a solar cell, but emulated by considering plastic substrates, was designed in [19] to achieve high optical transparency (about 93%). The design was developed at 2.61 GHz, with a fractional BW of 2.1%. More recently, CP and high transparency have been obtained in [20] by introducing two nearly square wired-based linear-polarized patch antennas rotated in space 90° from each other and fed 90° out of phase. In that work, a transparent

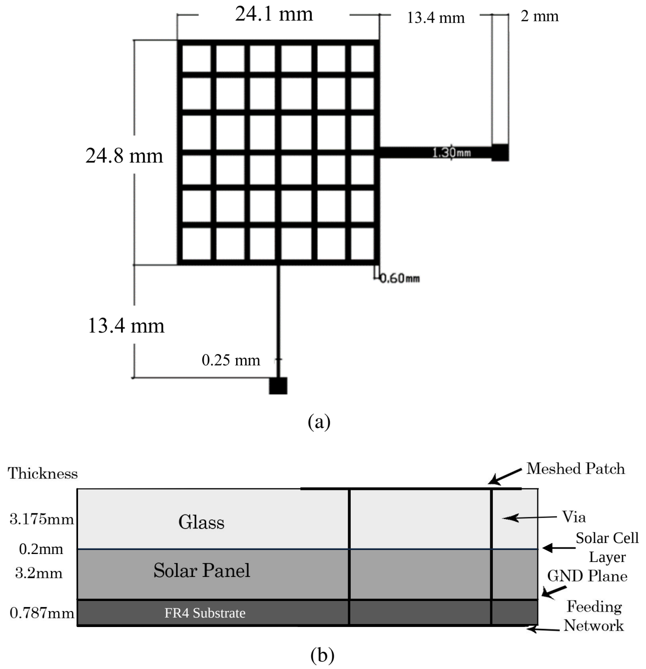

FIGURE 2. **(a) Meshed CP patch antenna top layout with relevant dimensions. (b) Cross-section view of the multilayer structure. It should be highlighted that the patch shares a ground (GND) plane with the bottom-side feeding circuit.**

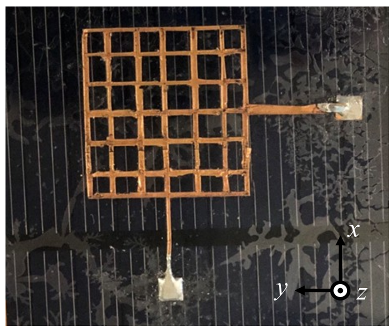

FIGURE 3. **Manufactured meshed patch antenna affixed to a silicon solar cell by interposing a borosilicate glass layer. The two feed points enabling CP operation are connected to the feed system (on the bottom side) using microstrip transmission lines and vias which penetrate through the solar panel.**

material (i.e., Lexan) was considered for the substrate, while only simulations were reported. The design enabled high transparency (about 80%) and a large operational BW (about 8.7%), at the cost of increased antenna size and thus reduced aperture efficiency. The ground plane of the antenna was also made by wires in [20] (to ensure reduced shadowing), but introduced some undesired back radiation. A CP antenna made by a nearly square meshed patch fed with a coplanar Y-shaped feed, but not integrated on a solar panel, has been proposed in [21]; whereas a uniform patch antenna integrated on a cubesat has been described in [22].

It should be mentioned that more conventional approaches to obtain CP for patch antennas (e.g., corner truncation or the use of slots) is not straightforward for the meshed patch. This can lead to complex and involved designs which might not be convenient to optimize and fabricate [15]. For example, designs in [15] reported that more circular patches and with a high degree of line width accuracy near the patch center were required. This resulted in a relatively narrow AR $BW_{3\,dB}$ of 2.79%, also due to the width of the grid lines, which were tapered differently along the patch surface to obtain the required degerante mode excitation. Therefore, more research efforts as reported in the litterature [16]- [20], are based on phase shift approaches to achieve CP for the meshed patch.

We propose here a simple and novel CP meshed patch (see Figs. 1-3) with a uniform ground plane and with two-port patch excitation for CP radiation, and with an integrated feed system, positioned underneath the silicon solar cells and the borosilicate layer. This improves the BW of the patch while also enhancing the broadside radiation; i.e., the measured radiating bandwidth and front-to-back ratio are about 13% and 20 dB, respectively, demonstrating enhanced performance with respect to the state of the art, as found in the literature and summarized above. Our proposed CP antenna also provides high transparency avoiding the use of thicker tapered lines and were the measured shadowing levels are below 10% over a 90° beam angle range enabling efficient solar cell operation. The structure is also simple to design and optimize and can be easily adapted to different satellite configurations and operating frequencies. Moreover, it can also provide dual-polarization features and can be used as a single element within an array for beam steering and other advanced satellite communications.

II. ANTENNA DESIGN APPROACH

The proposed meshed patch antenna was designed to operate at about 2.45 GHz but can be easily adapted to work at higher frequencies or with different technologies by tuning the patch dimensions and the substrate parameters. To achieve CP the antenna is fed by means of two vertical probes penetrating through the silicon solar cell and the transparent borosilicate glass layer (see Figs. 2 and 3). This is necessary to connect the feeding network and the radiating patch with the relevant communication electronics placed within the satellite structure.

A preliminary meshed-patch structure has been designed, manufactured, and tested using an FR4 material (see Fig. 4). The structure is very simple and based on standard PCB fabrication processes and has a thickness equal to 1.6 mm and relative permittivity $\varepsilon_{r,PCB} = 4.4$. The square patch sides are 25.25 mm long, the corresponding meshed lines have a width of 1 mm, and the size of the entire substrate is $0.5\lambda \times 0.5\lambda$.

The preliminary structure is excited by means of two microstrip transmission lines fed by SMA connectors. Fig. 4(a) reports both the measured and simulated reflection coefficient at the first port (similar results are observed for the second port, not shown for brevity). A minimum value equal to -19 dB at 2.385 GHz and a -10 dB impedance BW of 33 MHz (1.45%) have been achieved. Fig. 4(b) depicts the realized CP gain versus frequency, showing a peak value, for both the measurements and simulations, equal to more than 4 dB_{ic} at 2.4 GHz. A measured AR (not reported here for space limitations) of 0.78 dB at 2.4 GHz has also been observed. The radiation patterns are shown in Fig. 4(c), where both the right-handed circularly polarized (RHCP) and the left-handed circularly polarized (LHCP) components are depicted. Cross-polarization levels (i.e., LHCP) are more than 20 dB below the co-polarized maximum at broadside and the half-power beamwidth is equal to about 60°.

To further assess the feasibility of the proposed antenna structure integrated within a solar cell, we have adapted the preliminary FR4 design to a multilayer implementation made by a borosilicate glass layer placed above a silicon solar-cell (see Fig. 2). We consider an FR4 substrate but with a thickness of 3.2 mm and $\varepsilon_{r,PCB} = 4.4$ which typically defines commercially available solar panels. We also include in the simulation model an array of metal-wire lines embedded within the silicon layer (0.2 mm thick, see Fig. 3) required for the collection of the incident solar power.

The transparent borosilicate glass layer ($\varepsilon_{r,glass} = 4.6$) has a thickness of 3.175 mm, which was chosen to increase the BW as well as to add a layer of protection for the solar cell. The meshed patch dimensions are presented in Fig. 2(a), with the main patch area being 26.8×24.1 mm, whereas the width of the mesh grid lines have been reduced to 0.6 mm. Quarter-wave transmission lines are added between the patch and the feeding ports to improve the matching of the antenna. It should also be mentioned that different transmission lines widths and lengths were needed to feed each port of the antenna. This is because the small metallic wires within the solar-cell layer (for power harvesting) introduced some anisotropy. A ground plane (having thickness of 0.787 mm) was placed below the solar panel, which was penetrated by two vias connected to the top patch and the feed system (see Fig. 2(b)).

The feeding network was designed to provide the relevant power split and phase offset (i.e., 90°) required to achieve CP operation. In particular, the antenna is fed by means of a Wilkinson power divider (in conjunction with a delay line), which was placed below the ground plane resulting in a planar and fully integrated antenna. To compensate for the noted asymmetry of the panel (that is the cause of the mentioned substrate anisotropy since the propagation constant for the quasi-TEM microstrip line mode is different in the x and y directions) an additional optimization step to achieve uniform amplitude excitation, but delayed 90° for the two degenerate patch modes on the top layer, was performed (all results not reported for brevity). This resulted in an optimized delay line with an electrical length of 116° within the feeding circuit.

The top layer of the solar-panel integrated antenna is made by a metallic mesh having thickness equal to 0.1 mm and it is directly placed on a commercial panel. The layout consists in a silicon layer and an FR4 substrate (as defined in Fig. 2(b)) with dimensions equal to 76 × 127 mm. The implemented design can also be adapted for more complicated and expensive panels used for CubeSats and other satellites. Also, the top trace for the meshed patch prototype has been constructed

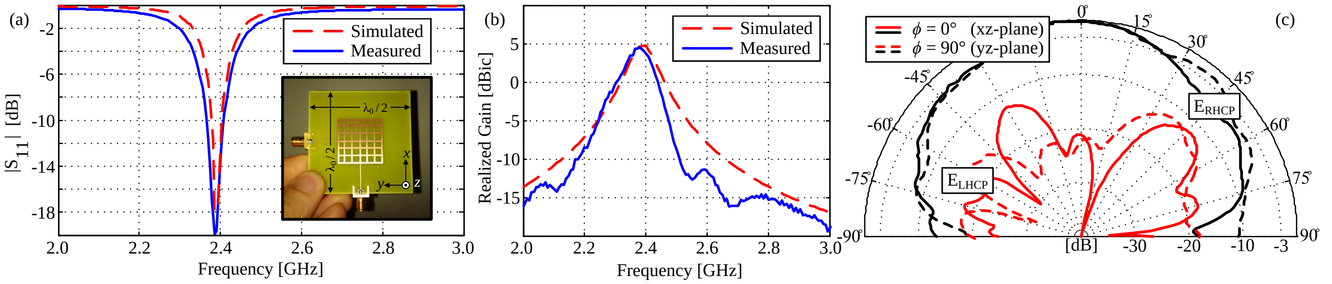

FIGURE 4. Results for the manufactured meshed CP patch antenna based on an FR4 substrate; i.e. the preliminary design: (a) simulated and measured impedance matching with a photo of the structure in the inset, (b) realized gain versus frequency where it can be observed that values are about 5 dB_{ic}, (c) measured radiation pattern in both the principal planes; cross-polarization levels (LHCP) are well below 20 dB from the main co-polarized broadside maximum.

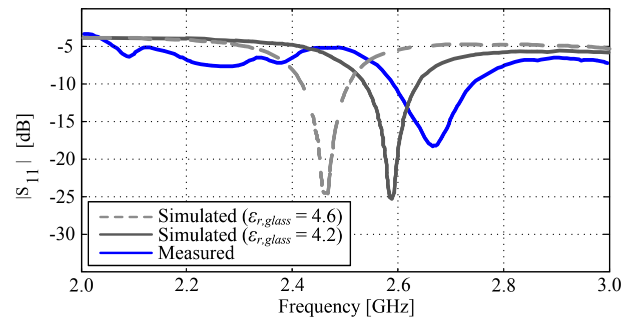

FIGURE 5. Impedance matching for the proposed meshed patch antenna (see Fig. 3). Results show agreement between the measurements and simulations when considering a relative dielectric constant of 4.2 (for the borosilicate glass layer) within the full-wave simulation model.

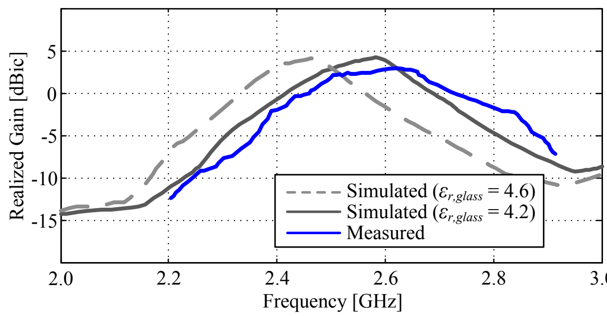

FIGURE 6. Realized gain at broadside versus frequency (values are above 0 dBic for about a 0.3 GHz BW). A similar $BW_{3\,dB}$ was also observed for the AR.

by means of conventional copper tape. A picture of the final and measured prototype can be seen in Fig. 3.

The performance of a similar multilayer antenna has been reported and discussed in [23] and will not be presented here. Those preliminary findings suggested that a peak gain value of 6.25 dB_{ic} and a minimum $|S_{11}|$ and $|S_{22}|$ at 2.4 GHz were equal to -20 dB. In that work, an AR equal to 0.68 dB was reported at the 2.4 GHz design frequency.

III. ANTENNA RESULTS AND DISCUSSIONS

To characterize the integrated antenna, measurements have been carried out using a calibrated anechoic chamber and a vector network analyzer. Any shadowing effects caused by the meshed patch have been tested using a lamp and a multimeter setup based on the same solar panel structure considering two scenarios, i.e., before placing the antenna on the top glass layer and integrating the antenna on the panel. Results and further explanations are reported from Figs. 5 to 9.

Fig. 5 reports both the simulated and measured reflection coefficient for the solar panel antenna prototype. A minimum at 2.45 GHz and 2.6 GHz equal to about -25 dB is shown for the simulated design with $\varepsilon_{\mathrm{r,glass}}$ = 4.6 and $\varepsilon_{\mathrm{r,glass}}$ = 4.2, respectively. These results correspond to an impedance BW of about 0.1 GHz centered at 2.45 GHz considering $|S_{11}| <$ -10 dB and $\varepsilon_{\mathrm{r,glass}}$ = 4.6. However, an upward frequency shift is observed for the measurements, likely due to permittivity tolerances for the borosilicate glass layer, which is a critical parameter for the antenna performance [19]. Also, the antenna was designed and optimized considering $\varepsilon_{\mathrm{r,glass}}$ = 4.6 for this glass layer, while measurements (both for the input impedance and realized gain, see Fig. 7) suggest an actual value equal to about 4.2. There could also be small modeling inconsistencies in the silicon solar panel layer

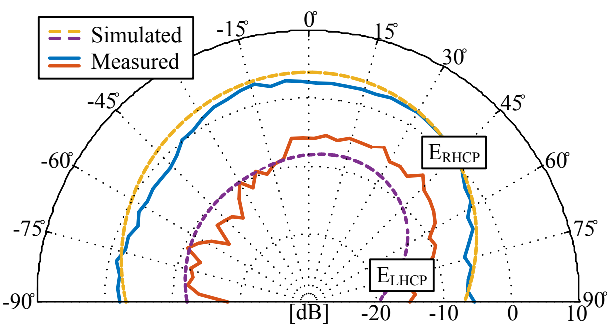

FIGURE 7. Beam pattern for the solar panel antenna design (see Fig. 3) where realized gain values are more than 2.5 dB_{ic}. It can be observed that the cross-polarization levels (LHCP) are about 10 dB below the main co-polarized maximum at broadside.

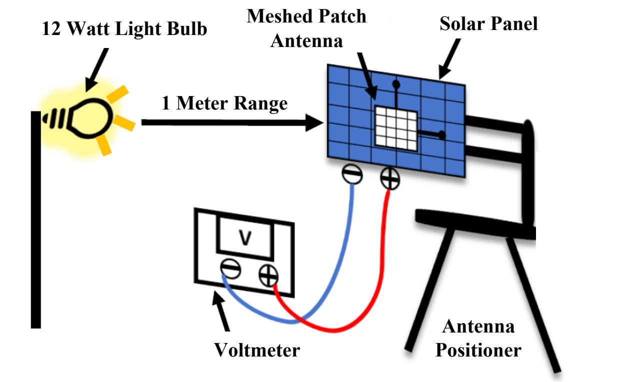

FIGURE 8. Experimental setup to determine the optical transparency (shadowing level) for the meshed patch. A 12 W source was positioned 1 m away from the solar panel and voltage levels versus angular position were recorded.

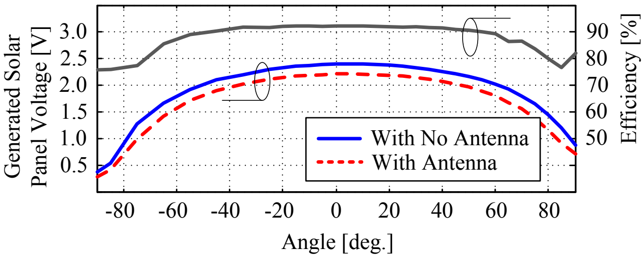

FIGURE 9. Measured potential difference generated at the solar panel (see Fig. 8) with and without the meshed patch antenna. Optical transparency values are well above 80% and 90% from about -70° to +80° and ±45°, respectively.

as compared to the fabricated prototype. In addition, some assembly tolerances when implementing the top patch could also explain the shift for the measured structure. Regardless of these practicalities, results for the manufactured prototype are in agreement with the simulations, demonstrating proof of concept.

Figs. 6 and 7 depict both the realized gain for the antenna as well as the simulated and measured beam pattern at 2.6 GHz whilst considering $\varepsilon_{\text{r,glass}}$ = 4.2 for the glass layer. The former reports a peak value of about 5 dB$_{ic}$ at 2.45 GHz and a measured value equal to more than 3 dB$_{ic}$. The difference between the measurements and simulations are likely the result of manufacturing inaccuracies and of the mentioned practicalities for the various involved layers.

A dedicated set of measurements to asses the effects of the meshed patch integrated on the solar panel voltage generation are also reported. The setup and the results are depicted in Figs. 8 and 9. As it can be observed, the harvested voltage for the solar panel with the meshed patch on top suffers a very limited reduction, i.e., less than 10% for most of the angles of illumination. This confirms the high transparency making the proposed design suitable for satellite implementations.

IV. CONCLUSION

In this paper, we have presented a novel configuration for a circularly polarized meshed patch antenna, whose structure and feeding network are fully integrated on a commercial solar panel. The design is optimized to save surface area aboard small satellites and to maximize the amount of solar power that is possible to collect. The compact size of the square patch makes it suitable for phased array applications and communications, both with other satellites and with the ground station. More importantly, to our knowledge, no similar CP prototype has been designed, manufactured, and tested.

The antenna is low-cost, compact and robust, and it can be easily adapted to any specific mission requirements. The most relevant features of the proposed structure, such as gain and impedance bandwidth, are competitive when compared with other antennas reported in the literature.

REFERENCES

[1] CubeSat Design Specification, rev. 13, available at http://www.cubesatorg., Apr. 2015.

[2] R. Martinez Rodriguez-Osorio and E. Fueyo Ramirez, "A hands-on education project: antenna design for inter-cubesat communications," IEEE Antennas Propag. Mag., vol. 54, no. 5, pp. 211–224, 2012.

[3] Y. Rahmat-Samii, V. Manohar, and J. M. Kovitz, "For satellites, think small, dream big: A review of recent antenna developments for cubesats," IEEE Antennas Propag. Mag., vol. 59, no. 2, pp. 22–30, Apr. 2017.

[4] T. Yekan and R. Baktur, "Conformal integrated solar panel antennas: Two effective integration methods of antennas with solar cells." IEEE Antennas Propag. Mag., vol. 59, no. 2, pp. 69–78, Apr. 2017.

[5] E. Pittella, S. Pisa, M. Pontani, A. Nascetti, P. D'Atanasio, A. Zambotti, and H. Hadi, "Reconfigurable s-band patch antenna system for cubesat satellites," IEEE Aerospace Electronic Sys. Mag., vol. 31, no. 5, pp. 6–13, 2016.

[6] S. Shynu, M. J. R. Ons, P. McEvoy, M. J. Ammann, S. J. McCormack, and B. Norton, "Integration of microstrip patch antenna with polycrystalline silicon solar cell," IEEE Trans. Antennas Prop., vol. 57, no. 12, pp. 3969–3972, 2009.

[7] N. Neveu, M. Garcia, J. Casana, R. Dettloff, D. R. Jackson, and J. Chen, "Transparent microstrip antennas for cubesat applications," in IEEE International Conference on Wireless for Space and Extreme Environments, Nov 2013, pp. 1–4.

[8] R. Garg, P. Bhartia, I. J. Bahl, and A. Ittipiboon, Microstrip antenna design handbook. Artech house, 2001.

[9] G. Clasen and R. Langley, "Meshed patch antennas," IEEE Trans. Antennas Prop., vol. 52, no. 6, pp. 1412–1416, 2004.

[10] A. Genc, T. Turpin, T. Yasin, and R. Baktur, "Active integrated meshed patch antennas for small satellites," Microwave Optical Tech. Lett, vol. 54, no. 7, pp. 1593–1595, 2012.

[11] S. Vaccaro, J. R. Mosig, and P. de Maagt, "Two advanced solar antenna" solant" designs for satellite and terrestrial communications," IEEE Trans. Antennas Prop., vol. 51, no. 8, pp. 2028–2034, Aug. 2003.

[12] R. Caso, A. D'Alessandro, A. Michel, and P. Nepa, "Integration of slot antennas in commercial photovoltaic panels for stand-alone communication systems," IEEE Trans. Antennas Prop., vol. 61, no. 1, pp. 62–69, 2013.

[13] T. R. Jones, J. P. Grey, and M. Daneshmand, "Solar panel integrated circular polarized aperture-coupled patch antenna for cubesat applications," IEEE Antennas Wireless Propag. Lett., vol. 17, no. 10, pp. 1895–1899, 2018.

[14] E. Escobar, N. Kirsch, G. Kontopidis, and B. Turner, "5.5 ghz optically transparent mesh wire microstrip patch antenna," Electronics Letters, vol. 51, no. 16, pp. 1220–1222, 2015.

[15] S. Sheikh, "Circularly polarized meshed patch antenna," IEEE Antennas Wireless Propag. Lett., vol. 15, pp. 352–355, 2016.

[16] T. Yasin and R. Baktur, "Circularly polarized meshed patch antenna for small satellite application," IEEE Antennas and Wireless Propagation Letters, vol. 12, pp. 1057–1060, 2013.

[17] ——, "Bandwidth enhancement of meshed patch antennas through proximity coupling," IEEE Antennas Wireless Propag. Lett., vol. 16, pp. 2501–2504, 2017.

[18] C. G. Ryan and G. V. Eleftheriades, “Single-and dual-band transparent circularly polarized patch antennas with metamaterial loading,” IEEE Antennas Wireless Propag. Lett., vol. 14, pp. 470–473, 2015.
[19] T. W. Turpin and R. Baktur, “Meshed patch antennas integrated on solar cells,” IEEE Antennas Wireless Propag. Lett., vol. 8, pp. 693–696, 2009.
[20] X. Liu, J. Liu, D. R. Jackson, J. Chen, P. W. Fink, and G. Y. Lin, “Broadband transparent circularly-polarized microstrip antennas for cubesats,” in 2016 IEEE International Symposium on Antennas and Propagation (APSURSI), June 2016, pp. 1545–1546.
[21] T. Yasin and R. Baktur, “Circularly polarized meshed patch antenna using coplanar y-shaped coupling feed,” Microwave and Optical Technology Letters, vol. 56, no. 2, pp. 487–489, 2014.
[22] T. Yekan and R. Baktur, “An x band patch antenna integrated with commercial triple-junction space solar cells,” Microwave and Optical Technology Letters, vol. 59, no. 2, pp. 260–265, 2017.
[23] B. K. Montgomery, S. K. Podilchak, and Y. M. Antar, “Circularly polarized meshed patch antenna for cubesats and other small sattelites,” in Proc. IEEE Int. Symp. Antennas Propap. IEEE, 2016, pp. 1547–1548.